bioRxiv preprint doi: https://doi.org/10.1101/2020.05.12.090068; this version posted June 19, 2020. The copyright holder for this preprint (which was not certified by peer review) is the author/funder, who has granted bioRxiv a license to display the preprint in perpetuity. It is made available under aCC-BY-NC-ND 4.0 International license.

Cell-extracellular matrix interactions in the fluidic phase direct the topology and polarity of self-organized epithelial structures

Mingxing Ouyang[1,2*], Jiun-Yann Yu[2], Yenyu Chen[2], Linhong Deng[1], Chin-Lin Guo[2*]

[1]Institute of Biomedical Engineering and Health Sciences, Changzhou University, Changzhou, Jiangsu Province, 213164 China

[21]Department of Bioengineering, California Institute of Technology, MS 138-78, 1200 E. California Blvd, Pasadena, CA 91125 USA

*To whom correspondence should be addressed:

Dr. Chin-Lin Guo

Current address: Associate Fellow at Institute of Physics, Academia Sinica,
128 Sec 2 academia road, NanKang District, Taipei, Taiwan 11579
Email: guochin@phys.sinica.edu.tw
Phone: 886-2-2789-6771

Dr. Mingxing Ouyang

Professor at Institute of Biomedical Engineering and Health Sciences, Changzhou University
1 Gehu Road, Wujin District, Changzhou City, Jiangsu Province 213164 China
Email: mxouyang@cczu.edu.cn
Phone: 086-0519-86330103

Running title: Extracellular matrix directs the topology and polarity of epithelium

bioRxiv preprint doi: https://doi.org/10.1101/2020.05.12.090068; this version posted June 19, 2020. The copyright holder for this preprint (which was not certified by peer review) is the author/funder, who has granted bioRxiv a license to display the preprint in perpetuity. It is made available under aCC-BY-NC-ND 4.0 International license.

Abstract

In vivo, cells are surrounded by extracellular matrix (ECM). To build organs from single cells, it is generally believed that ECM serves as a large-scale scaffold to coordinate cell positioning and differentiation. Nevertheless, how cells utilize cell-ECM interactions to spatiotemporally coordinate their positioning and differentiation to different ECM at the whole-tissue scale is not fully understood. Here, using *in vitro* assay with engineered MDCK cells co-expressing H2B-mCherry (nucleus) and gp135 (Podocalyxin)-GFP (apical marker), we show that such spatiotemporal coordination for epithelial morphogenesis and polarization can be initiated and determined by cell-soluble ECM interaction in the fluidic phase. The coordination depends on the native topology of ECM components such as sheet-like basement membrane (BM, mimicked by Matrigel in experiments) and linear fiber-like type I collagen (COL). Two types of coordination are found: scaffold formed by BM (COL) facilitates a close-ended (open-ended) coordination that leads to the formation of lobular (tubular) epithelium, where polarity is preserved throughout the entire lobule/tubule. During lobular formation with BM, polarization of individual cells within the same cluster occurs almost simultaneously, whereas the apicobasal polarization in the presence of COL can start at local regions and proceed in a collective way along the axis of tubule, which might suggest existence of intercellular communications at the cell-population level. Further, in the fluidic phase, we found that cells can form apicobasal polarity throughout the entire lobule/tubule without a complete coverage of ECM at the basal side. Based on reconstructions from time-lapse confocal imaging, this is likely derived from polarization occurring at early stage and being maintained through growth of the epithelial structures. Under suspension culture with COL, the polarization was impaired with formation of multi-lumens on the tubes, implying the importance of ECM microenvironment for

bioRxiv preprint doi: https://doi.org/10.1101/2020.05.12.090068; this version posted June 19, 2020. The copyright holder for this preprint (which was not certified by peer review) is the author/funder, who has granted bioRxiv a license to display the preprint in perpetuity. It is made available under aCC-BY-NC-ND 4.0 International license.

tubulogenesis. Our results suggest a mechanism for cells to form polarity and coordinate positioning *in vivo*, and a strategy for engineering epithelial structures through cell-soluble ECM interaction and self-assembly *in vitro*.

Keywords: epithelial self-assembly; tubulogenesis; type I collagen; fluidic phase; cell-ECM interaction; epithelial polarity

Introduction

An amazing feature in epithelial development and regeneration is the spatiotemporal coordination of cell positioning and differentiation[1]. In these processes, cells develop apicobasal polarity and form lobular or tubular sheets[2; 3]. Most remarkably, they can coordinate the orientation of polarity throughout the entire tissue[3]. Loss of such coordination is often a hallmark of tumors[4]. As such, understanding how epithelial cells coordinate their positioning and polarization is not only essential for developmental biology and regenerative medicine, but also important for cancer biology. The transmembrane glycoprotein gp135 (also called Podocalyxin) is often used as an apical marker located at the luminal surfaces[5; 6], and Rab small GTPases mediate the direct transportation of gp135 and apicobasal polarization[7; 8]. Over the past few decades, studies on epithelial morphogenesis have indicated the importance of cell-cell adhesions and cell-extracellular matrix (ECM) interactions[5; 9; 10; 11; 12; 13; 14; 15; 16]. In particular, the differentiation of epithelial cells in which non-polarized cells form polarized epithelium depends on ECM components[12]. It was shown that breast epithelial cells differentiate into tubules in type I collagen (COL)[17; 18], while they form lobular acini in basement membrane (BM, mimicked by Matrigel in experiments)[19; 20]. Our previous study further showed that cell-collagen interaction permits a long-range morphogenetic coordination at

bioRxiv preprint doi: https://doi.org/10.1101/2020.05.12.090068; this version posted June 19, 2020. The copyright holder for this preprint (which was not certified by peer review) is the author/funder, who has granted bioRxiv a license to display the preprint in perpetuity. It is made available under aCC-BY-NC-ND 4.0 International license.

sub-millimeter scale[21]. Nevertheless, how epithelial cells utilize cell-ECM interaction to coordinate their positioning and polarization in response to different ECM components at the whole-tissue scale is not fully understood.

To form long-range coordination, it is generally believed that ECM can serve as scaffolds to guide cell positioning and polarization[16]. Cells constantly secrete soluble ECM molecules and degrade existing ECM scaffolds into soluble fragments *in vivo*. Theoretically, these soluble forms of ECM can be assembled into scaffolds through two processes. The first is that they self-assemble into new scaffolds or re-incorporate into pre-existing scaffolds. Alternatively, soluble ECM can interact with cells which serve as nucleation cores to assemble ECM scaffolds. An example is the development of renal tubules where BM components are found to be dynamically assembled around the pre-tubular structure[22]. Apicobasal polarization is a typical process during epithelial tubulogenesis, and consistently with the role from ECM, the cellular mechanism involving integrin and RhoA signaling pathways has been identified in triggering the polarity formation[23; 24].

Here, we study whether ECM scaffolds created by ECM self-assembled hydrogel or by cell-mediated assembly play the primary roles in the formation and coordination of epithelial morphogenesis. These two processes can hardly be decoupled *in vivo* or through the conventional 3-D ECM reconstitution approaches. Our recent work demonstrated that cell motion promotes fibrillary assembly of soluble COL, in supporting the role of cells in ECM scaffold generation[25]. We therefore use the *in vitro* open-system assay, and found that spatiotemporal coordination in epithelial morphogenesis and polarization can occur on cell-assembled ECM in the fluidic phase rather than pre-assembled ECM in the solid phase. The coordination depends on native topology of the ECM components such as basement membrane

bioRxiv preprint doi: https://doi.org/10.1101/2020.05.12.090068; this version posted June 19, 2020. The copyright holder for this preprint (which was not certified by peer review) is the author/funder, who has granted bioRxiv a license to display the preprint in perpetuity. It is made available under aCC-BY-NC-ND 4.0 International license.

(BM) and type I collagen (COL). Further discovered during tubulogenesis, the apicobasal polarization is initiated at local regions and proceeds in a collective way along the axis of the tubule, implying intercellular communications within the cell groups. Our results suggest a potential mechanism which cells can use to form polarity and coordinate morphogenesis *in vivo*, and a strategy to engineer epithelial structures through self-assembly *in vitro*.

Results

Cell-ECM interactions in the fluidic phase for polarized epithelium formation

We first examined if cells can develop coordinated polarity on ECM scaffolds formed by ECM self-assembly without any soluble ECM. Madin-Darby Canine Kidney (MDCK) cells were used in this study, which are a popular model cell line for epithelial morphogenesis and apicobasal polarity formation regulated by Rab GTPases[3; 8]. To track the development of apicobasal polarity, we engineered MDCK cells stably expressing mCherry-conjugated histone H2B (H2B-mCherry) and GFP-conjugated gp135 (gp135-GFP). Here, H2B-mCherry is used to indicate cell nucleus[26], whereas the apical marker gp135 is used to indicate cell polarization[5; 27]. To define polarity, we noted that in polarized 3-D epithelium, cells are organized into a surrounding and continuous monolayer structure with gp135 primarily confined at their apical surfaces[5], which are located at the inner space of the organization (illustrated in Fig. 1a with the experimental data shown in Fig. 1b-d). Thus, we used the spatial distribution of H2B-mCherry with respect to gp135-GFP to define and track the formation of polarity. To initiate cell density-dependent long-range coordination, we adopted the cell density characterized and optimized in our previous study [21].

bioRxiv preprint doi: https://doi.org/10.1101/2020.05.12.090068; this version posted June 19, 2020. The copyright holder for this preprint (which was not certified by peer review) is the author/funder, who has granted bioRxiv a license to display the preprint in perpetuity. It is made available under aCC-BY-NC-ND 4.0 International license.

After long-term culture, epithelial cells including MDCK cells can secrete ECM molecules[10; 28; 29]. We therefore used open systems to dilute and/or remove secreted ECM by changing medium every day or every other day. Cells were cultured on pre-assembled BD Matrigel gels (to mimicking basement membrane (BM), the primary matrix components underlying polarized epithelium *in vivo*) open to a large medium space that contained no soluble ECM (Fig. 1a). Under this condition, cells grew and merged into big clusters (hundreds of micrometers in diameter) without forming general apicobasal polarity (Fig. 1b, top row). In order to visualize the cultured epithelium, 3-D projection of the epifluorescence images taken at 21 planes with a step size 4.5 μm was obtained by collecting pixels with the maximal intensity through the entire z-stack into a single plane, which is further explained in the Methods.

We then examined if cell-ECM interactions in the fluidic phase is required for polarity formation. Two types of medium were prepared: medium with BM (2%, diluted Matrigel solution from ~10 mg/ml stock concentration), and medium with COL (20 μg/ml). From the manufacturer, the major components of Matrigel are laminin (~61%), collagen IV (~30%) and Entactin (~7%). The BM concentration was adapted from studies by our group and others [7; 12; 20; 21; 23], and the COL concentration at 20 μg/ml was designed to match the similar mass concentration of 2% BM. Here, we used low concentrations of soluble ECM components to prohibit their fast self-assembly into hydrogel-like. This allowed cells to live in a fluidic or semi-fluidic condition and interact with soluble ECM during their proliferation. Here semi-fluidic condition referred to cells/clusters culturing on solid Matrigel scaffold with direct exposure to the medium. In response to soluble BM, cells were found to form spherical, lobular structures with coordinated polarity (Fig. 1b, middle row), whereas for soluble COL, they formed polarized, tubular structures (Fig. 1b, bottom row). In both cases, gp135 was confined within the apical area (Fig.

bioRxiv preprint doi: https://doi.org/10.1101/2020.05.12.090068; this version posted June 19, 2020. The copyright holder for this preprint (which was not certified by peer review) is the author/funder, who has granted bioRxiv a license to display the preprint in perpetuity. It is made available under aCC-BY-NC-ND 4.0 International license.

1b, middle and bottom rows, right). 3-D view of these cultured lobular and tubular structures from confocal scanning microscopy further confirmed that cells grew into fine 3-D structures with gp135 confined at the apical surfaces (Fig. 1c&d).

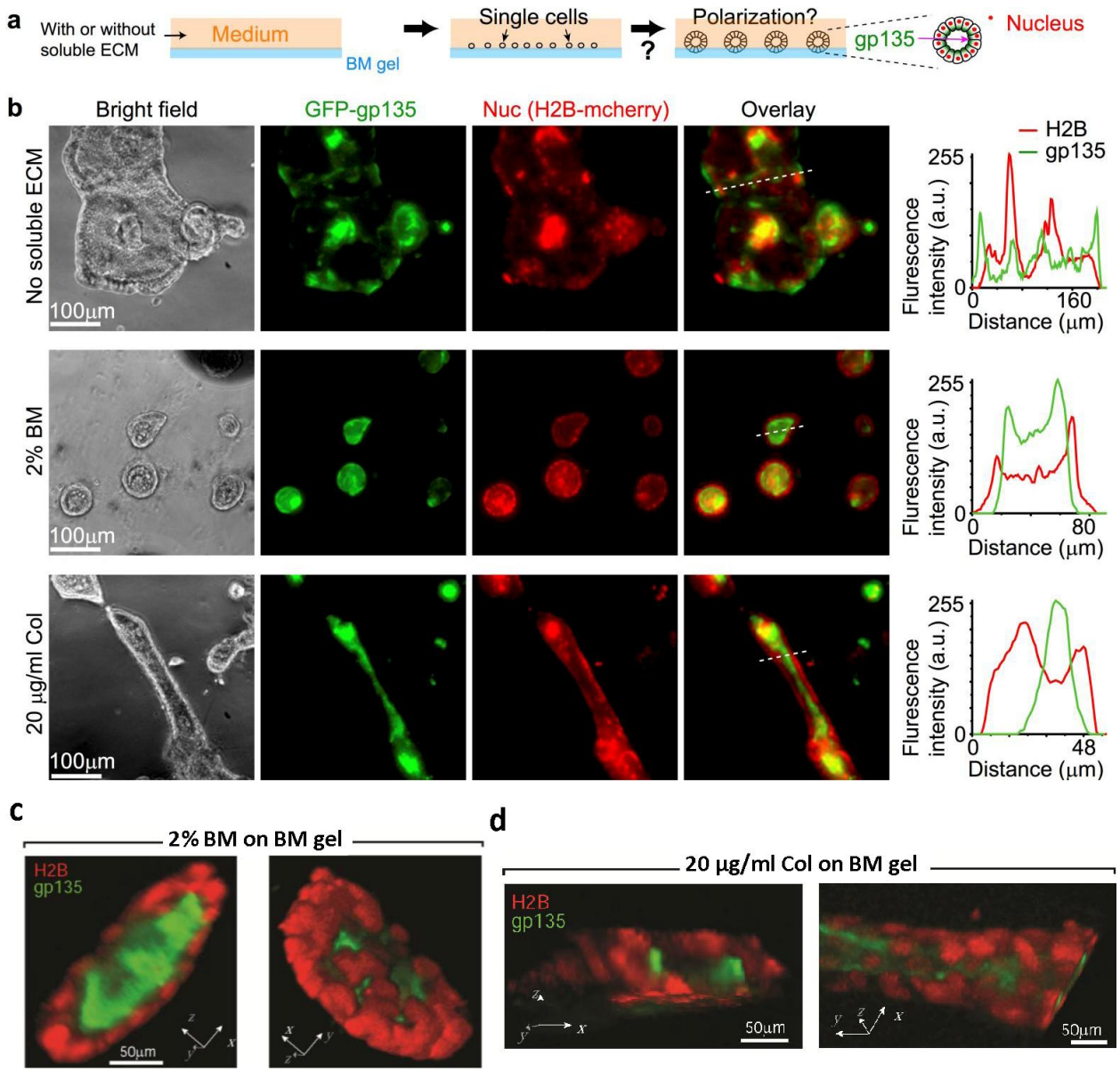

Figure 1 | Soluble ECM components are required to form epithelial polarization on Matrigel. (a) Experimental setup. MDCK cells were cultured on the top of basement membrane (BM) gels with or without soluble ECM components in the medium. Cells express H2B-mCherry

bioRxiv preprint doi: https://doi.org/10.1101/2020.05.12.090068; this version posted June 19, 2020. The copyright holder for this preprint (which was not certified by peer review) is the author/funder, who has granted bioRxiv a license to display the preprint in perpetuity. It is made available under aCC-BY-NC-ND 4.0 International license.

and gp135-GFP to indicate their nucleus and polarity, respectively. Note the distribution of nucleus with respect to gp135 in polarized lumens (on the right). **(b)** Left in each row: Represented phase contrast (bright field) and 3-D projected fluorescent images (gp135: green, H2B: red, and their overlay) for cells seeded on BM gels and cultured for 12 days. The medium contained (top row) no soluble ECM, (middle row) 2% BM, or (bottom row) 20 μg/ml type I collagen (COL). Nuc: cell nucleus. Right in each row: Fluorescence intensities of H2B-mCherry and gp135-GFP along the indicated white dotted lines (from left to right). The overlay of the red and green curves indicates the positions of cell nucleus (red) with respect to the apical marker (green). a. u.: arbitrary unit. Initial cell density: $1\text{-}2\times10^4/cm^2$, adapted from [21]. **(c & d)** 3-D view of the polarized lobular and tubular structures. The images from confocal scanning microscopy (with 20x objective) were reconstructed into 3-D structures. The 3-D views from different angles showed the relative position of cell nucleus (red) and apical marker gp135 (green) in the closed lobular (c) and elongated tubular (d) structures.

Dynamics of cell positioning and polarization dependent on cell-ECM interactions

Having shown that cell-BM (COL) interactions in the fluidic phase leads to the formation of polarized lobules (tubules), we examined how cells coordinate their positioning and polarization in response to soluble BM (COL). Same as the setups in Fig. 1a, cells were seeded on 3-D BM with or without soluble ECM in the medium (Fig. 2a), and the dynamic processes of cell aggregation and polarization were continuously recorded by time-lapse imaging in the following days (Fig. 2b with representative data shown in Fig. 2c-f).

bioRxiv preprint doi: https://doi.org/10.1101/2020.05.12.090068; this version posted June 19, 2020. The copyright holder for this preprint (which was not certified by peer review) is the author/funder, who has granted bioRxiv a license to display the preprint in perpetuity. It is made available under aCC-BY-NC-ND 4.0 International license.

We first examined cellular dynamics on BM gels in the presence or absence of soluble BM. Without soluble BM, time-lapse microscopy revealed that individual cells proliferated into small clusters, which continuously grew and merged with each other without general polarity formation (through the 5-day period of observation, Movie 1) (Fig. 2c, Movie 1). By contrast, with soluble BM, most clusters (> 90%) stopped merging and became polarized on the 2nd-3rd day (with the starting day as Day 0) (Fig. 2d). Here, the timing of polarization was defined by the conversion of gp135 from the outer layers to the inner areas of clusters/cysts (Fig. 2d, and Movie 2). During the polarization, most clusters (> 90%) were found to continuously expand through cell division but not through cluster coalescence (Movie 2). The lumen cultured by MDCK cells (H2B-mCherry/GFP-β-actin) displays actin ring at the apical side (Fig. 2e), which was consistent with the previous report[30].

We next examined the cellular dynamics on BM gels with soluble COL. Similar to the observation with soluble BM (Fig. 2d), cells were found to form clusters which proliferated and coalesced. However, the coalescence did not stop on the 3rd day but instead continued till most clusters/cysts (> 90%) fused into a long-range (>200 μm), tubule-like structure (Fig. 2f). By then, cells started to polarize through a collective conversion of gp135 from the outer layer to the inner area of tubule (Fig. 2f, Movie 3). It is noted that unlike the case with soluble BM where polarization of individual cells within the same cluster occurred almost simultaneously (Movie 2), the polarization in the presence of soluble COL started at some local regions and proceeded collectively along the axis of tubule in the same cluster (Fig. 2g, Movie 3). As fluorescence quantification shown on the right of Fig. 2g, in respect to the cell nuclei position (ΔL_n), the spatial localization of gp135 (ΔL_g) started to turn over from the boundary to the center of the tube along the polarization process. During the coalescence, we often observed mutual attraction of

bioRxiv preprint doi: https://doi.org/10.1101/2020.05.12.090068; this version posted June 19, 2020. The copyright holder for this preprint (which was not certified by peer review) is the author/funder, who has granted bioRxiv a license to display the preprint in perpetuity. It is made available under aCC-BY-NC-ND 4.0 International license.

clusters on the field of views under the time-lapse microscopy (Movie 3). Such interaction and prolonged coalescence was not observed in the case where cells were surrounded with soluble BM, suggesting that it is a feature of COL-cell interactions.

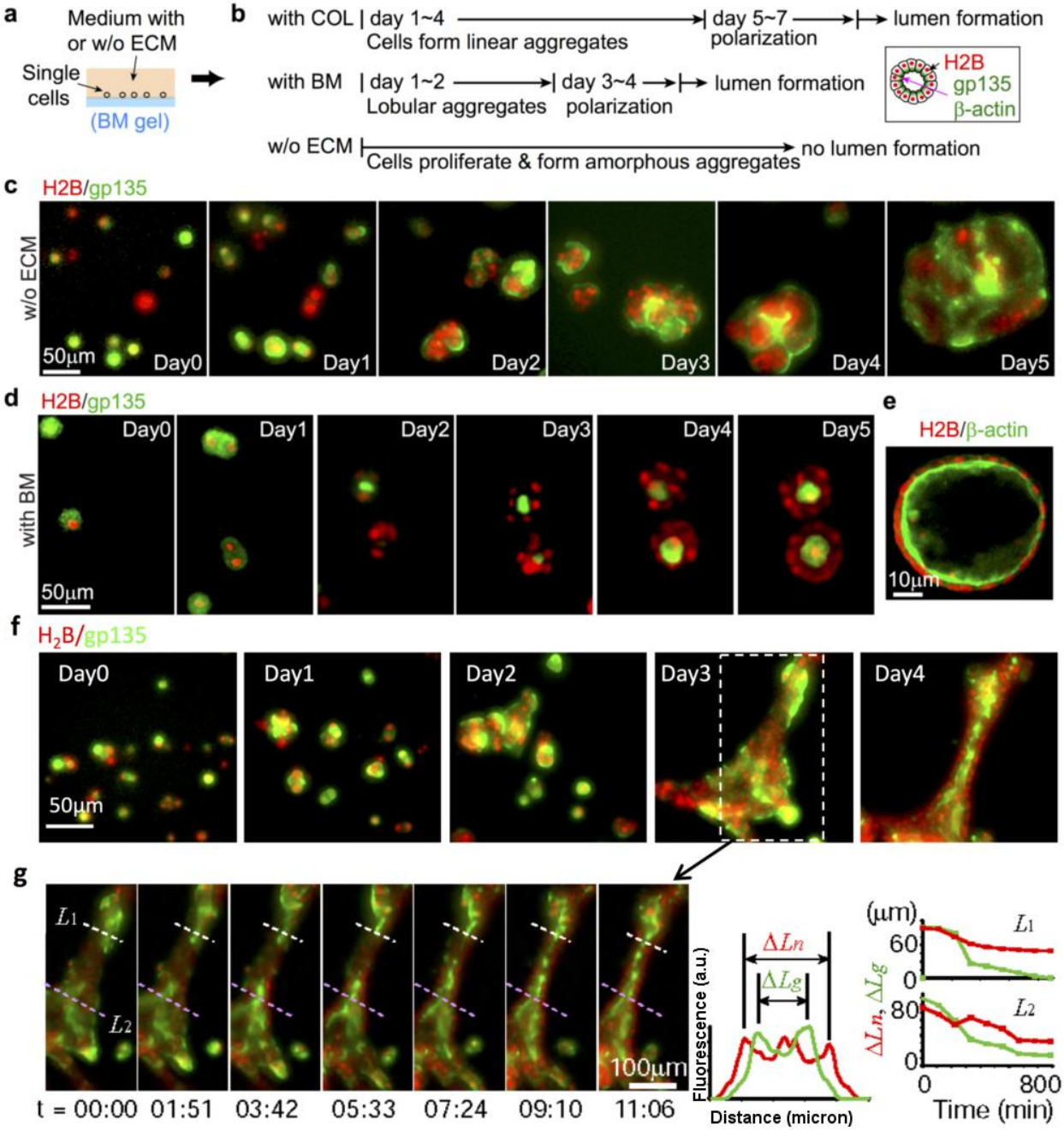

bioRxiv preprint doi: https://doi.org/10.1101/2020.05.12.090068; this version posted June 19, 2020. The copyright holder for this preprint (which was not certified by peer review) is the author/funder, who has granted bioRxiv a license to display the preprint in perpetuity. It is made available under aCC-BY-NC-ND 4.0 International license.

Figure 2 | Distinct dynamics of cell coordination in response to soluble BM/COL. **(a)** Experimental setup. MDCK cells were cultured on the top of basement membrane (BM) gels with or without ECM in the medium. **(b)** The observed results in different conditions (initial cell density: 1-2 $\times 10^4/cm^2$). Cells express H2B-mCherry and GFP-gp135 or β-actin-GFP to indicate cell nucleus and apicobasal polarity, respectively. Inlet: the distribution of nucleus with respect to gp135 / β-actin in polarized lumen. The first day was set as Day 1 in this schematic view. **(c & d)** Represented time series of 3-D projected epifluorescence images (gp135: green, H2B: red) for cells in medium (c) without ECM, (d) with 2% basement membrane (BM) components (also seen in Movies 1&2, interval = 22 min). **(e)** Represented optical sectioning from scanning microscopy (β-actin: green, H2B: red) to demonstrate lumen formation with polarized actin distribution after culturing cells in medium containing 2% BM for 14 days. **(f)** Represented time series of 3-D projected epifluorescence images for cells in medium with 20 μg/ml type I collagen (COL) (also seen in Movie 3, interval = 22 min). **(g)** The collective apicobasal polarization at cell-population level during tubulogenesis. The time-sequence images (left) from the sample (f) showed the collective polarization process along the tubular axis. The fluorescence quantification along the lines (L_1, L_2) (right) showed the spatial distribution of gp135 (green curves) relative to cell nuclei (H2B, red curves) during the polarization. ΔLn and ΔLg refer to the distances of boundary nuclei (H2B) and gp135 respectively crossing the tube, which were based on two peaks of their fluorescence measurements on the lines (L_1, L_2).

Cell polarization in the fluidic phase with ECM assembly

bioRxiv preprint doi: https://doi.org/10.1101/2020.05.12.090068; this version posted June 19, 2020. The copyright holder for this preprint (which was not certified by peer review) is the author/funder, who has granted bioRxiv a license to display the preprint in perpetuity. It is made available under aCC-BY-NC-ND 4.0 International license.

If the coordination of cell positioning and polarization requires the formation of ECM scaffolds, the results above suggest that it is the scaffold mediated by cell-ECM interaction in the fluidic phase that determines epithelial morphology and coordinates epithelial polarity. To see how such scaffolds are formed and affect cell positioning and polarization, we performed immuno-staining of laminin (a major component in BM[31]) and type I collagen (COL) on polarized lobules and tubules.

We first examined how laminin is distributed on cells seeded on BM gels with or without soluble BM. In the presence of soluble BM, condensed laminin was found at the outer layers of clusters after 3 days of culture (Fig. 3a), roughly the time by which most clusters stopped merging (Fig. 3d, and Movie 2). The density of laminin increased with time. After 7 days, most clusters (>95%) were found to form polarized lobules surrounded by dense laminin (Fig. 3a). By contrast, laminin was not found at the outer layers of clusters in the absence of soluble BM (Fig. S1), where clusters continuously grew and coalesced without polarity formation (Movie 1), suggesting that laminin assembled around clusters might block coalescence and induce polarization.

In the conventional model, the development of epithelial apicobasal polarity requires coordinated cell-ECM interaction at the basal side [9; 32] and cell-cell interactions [2; 13] at the lateral side of each individual cell. To ascertain if this is the case in our in vitro assays where cell-ECM interactions at the fluid phase appeared to play the deterministic role in apicobasal polarity formation, we examined the distribution of laminin around the clusters undergoing polarization. Cells on BM gels were cultured for 12 days with soluble BM to form polarized lobular lumens. Confocal scanning microscopy was then performed to construct 3-D views of laminin and lumens with the lumens outlined by H2B-mCherry signal from cell nucleus. Surprisingly, no

bioRxiv preprint doi: https://doi.org/10.1101/2020.05.12.090068; this version posted June 19, 2020. The copyright holder for this preprint (which was not certified by peer review) is the author/funder, who has granted bioRxiv a license to display the preprint in perpetuity. It is made available under aCC-BY-NC-ND 4.0 International license.

complete, uniform assembly of laminin around the lobular lumens was found. Instead, assembled laminin was found to form a lateral platform at the lateral side of each lumen, rather than on the top (facing the medium) or bottom (facing the BM gel) (Fig. 3c, and Movie 4; fluorescence intensities of laminin at the top and bottom of lobules were compatible with background), whereas cells at the entire lumen were polarized (Fig. 3d, which 3-D view is shown in Fig. 1c). These results also suggest that cells at the top of lumen could polarize in the absence of direct cell-ECM contact. The laminin platform appears as a 2-D network compatible with the native topology of BM[33]. Figure 3e depicts the spatial relation between the polarized lobular lumens and the assembled laminin network.

To see if cells can also polarize without direct cell-ECM contact in the presence of soluble COL, we examined the distribution of COL around the clusters that underwent polarization on BM gels with soluble COL in the medium. After 12 days of culture, cells formed tubules and found associated with linear structures of COL (Fig. 3f, pink arrow). Confocal scanning microscopy revealed that COL was condensed at the lateral sides, but not the top or bottom of tubules (Fig. 3g), yet similar to the results in the case with soluble BM (Fig. 3d), cells at the entire tubules were polarized (Fig. 3f). Since cells did not form polarity without soluble ECM (Fig. 1b, and Movie 1), it is likely that cell-ECM interactions in the fluidic phase can nucleate a scaffold to initiate polarity formation.

bioRxiv preprint doi: https://doi.org/10.1101/2020.05.12.090068; this version posted June 19, 2020. The copyright holder for this preprint (which was not certified by peer review) is the author/funder, who has granted bioRxiv a license to display the preprint in perpetuity. It is made available under aCC-BY-NC-ND 4.0 International license.

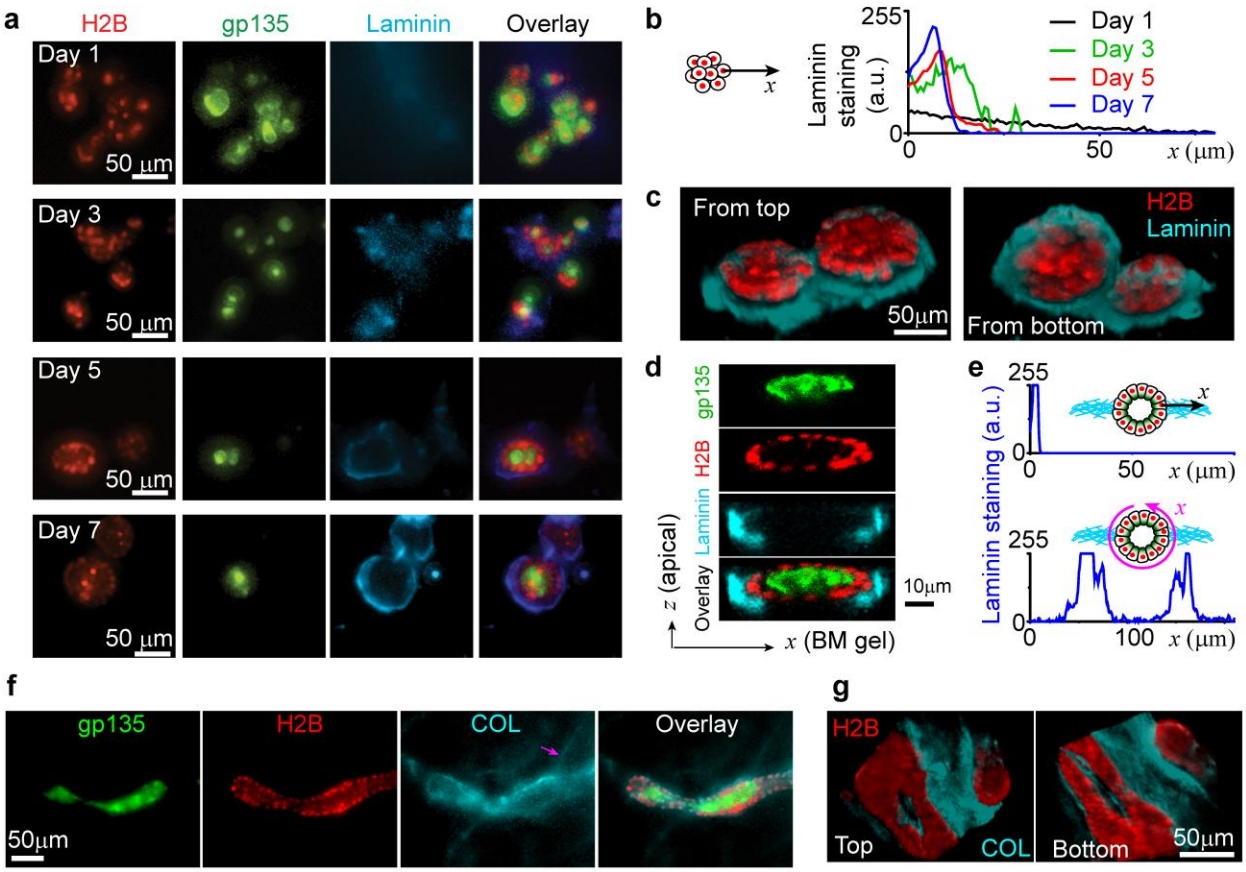

Figure 3 | Cell polarization in the fluidic phase with and without direct cell-ECM contact. **(a, b)** Lateral assembly of laminin around the luminal structure. MDCK cells were cultured for 1-7 days on BM gels with 2% BM in the medium, followed by the immuno-staining of laminin. (a) Represented fluorescent images of gp135-GFP (green), H2B-mCherry (red), laminin staining (cyan), and their overlay. (b) Fluorescence quantification of laminin staining on the boundaries of cultured MDCK clusters (a). **(c)** Represented images of 3-D reconstructed, top and bottom views of cell nucleus (red) and laminin (cyan) (also seen in Movie 4). Note the lateral condensation of laminin around the lobules (outlined by nucleus) and the absence of laminin assembly on the top and bottom of lobules. **(d)** Cross-section of the polarized epithelial lobules displaying cell nuclei (H2B), gp135 at the apical side, and laminin staining partially at the lateral

bioRxiv preprint doi: https://doi.org/10.1101/2020.05.12.090068; this version posted June 19, 2020. The copyright holder for this preprint (which was not certified by peer review) is the author/funder, who has granted bioRxiv a license to display the preprint in perpetuity. It is made available under aCC-BY-NC-ND 4.0 International license.

side. **(e)** Fluorescence quantification of laminin staining on the lobule (d) along the x-pointing direction from cell nuclei toward outside (up) or surrounding the lobular structure (below). **(f)** Represented fluorescent images of gp135-GFP (green), H2B-mCherry (red), COL staining (cyan), and their overlay. MDCK cells were cultured for 12 days on BM gels with COL (20 μg/ml) in the medium, followed by the immuno-staining of COL. Note the formation of linear structure of COL (pink arrow). **(g)** Represented images of 3-D reconstructed, top and bottom views of cell nucleus (red) and COL (cyan). Note the lateral condensation of COL around the tubules (outlined by nucleus) and the absence of COL assembly on the top and bottom of tubules. For (c & g), images were taken by confocal scanning microscope and created by ImageJ 3-D reconstructions.

The expansion of dividing cells into fine lobular structure under polarization

To further understand how cells maintained apicobasal polarity at the entire epithelial structures with only partial cell-ECM interactions during the culture, we carried time-lapse confocal imaging to observe the growth of dividing cells into polarized lobules. This experiment had certain technical challenges: due to the smaller size of each field by confocal imaging than the wide-field epi-microscopy, the motile cell samples could move out of the views more likely; second, confocal imaging had higher photo-toxicity during the point-by-point scanning and z-stack imaging, which could cause damage on cell samples. To manage to get some time-lapse samples successfully, we tried to lower the excitation laser power (25 mW) and used long interval time (3 or 4 hours).

bioRxiv preprint doi: https://doi.org/10.1101/2020.05.12.090068; this version posted June 19, 2020. The copyright holder for this preprint (which was not certified by peer review) is the author/funder, who has granted bioRxiv a license to display the preprint in perpetuity. It is made available under aCC-BY-NC-ND 4.0 International license.

As the cell cluster growth shown in Fig. 4 with more detailed views in Movie 5, the cell sample started at two-cell stage, and continued to divide into 3 and 4-cell cluster without polarization (located on one plane) on the next day; late on the third day, the polarization occurred in one cluster (not sure whether the same one from the beginning), and in the following days, the cluster continued to grow and expand into fine 3-D lobular structure with maintained polarization, suggesting the possibility of cell divisions occurred under polarized status in the lobule. These time-sequence images indicate that the cell cluster got polarized at early stage, and grew into fine-constructed 3-D lobule under maintained polarization. The result may help explain how cell polarization occurred on the entire lobules although there was only partial laminin coverage on the basal side (Fig. 3c-d). Similar mechanism may be extended to the observed tubular structure with partial COL coverage (Fig. 3f&g). In considering that this is a descriptive data with limited work, we didn't have explanation why ECM components weren't assembled on the top of the lobule, or dig out more insights at current stage.

bioRxiv preprint doi: https://doi.org/10.1101/2020.05.12.090068; this version posted June 19, 2020. The copyright holder for this preprint (which was not certified by peer review) is the author/funder, who has granted bioRxiv a license to display the preprint in perpetuity. It is made available under aCC-BY-NC-ND 4.0 International license.

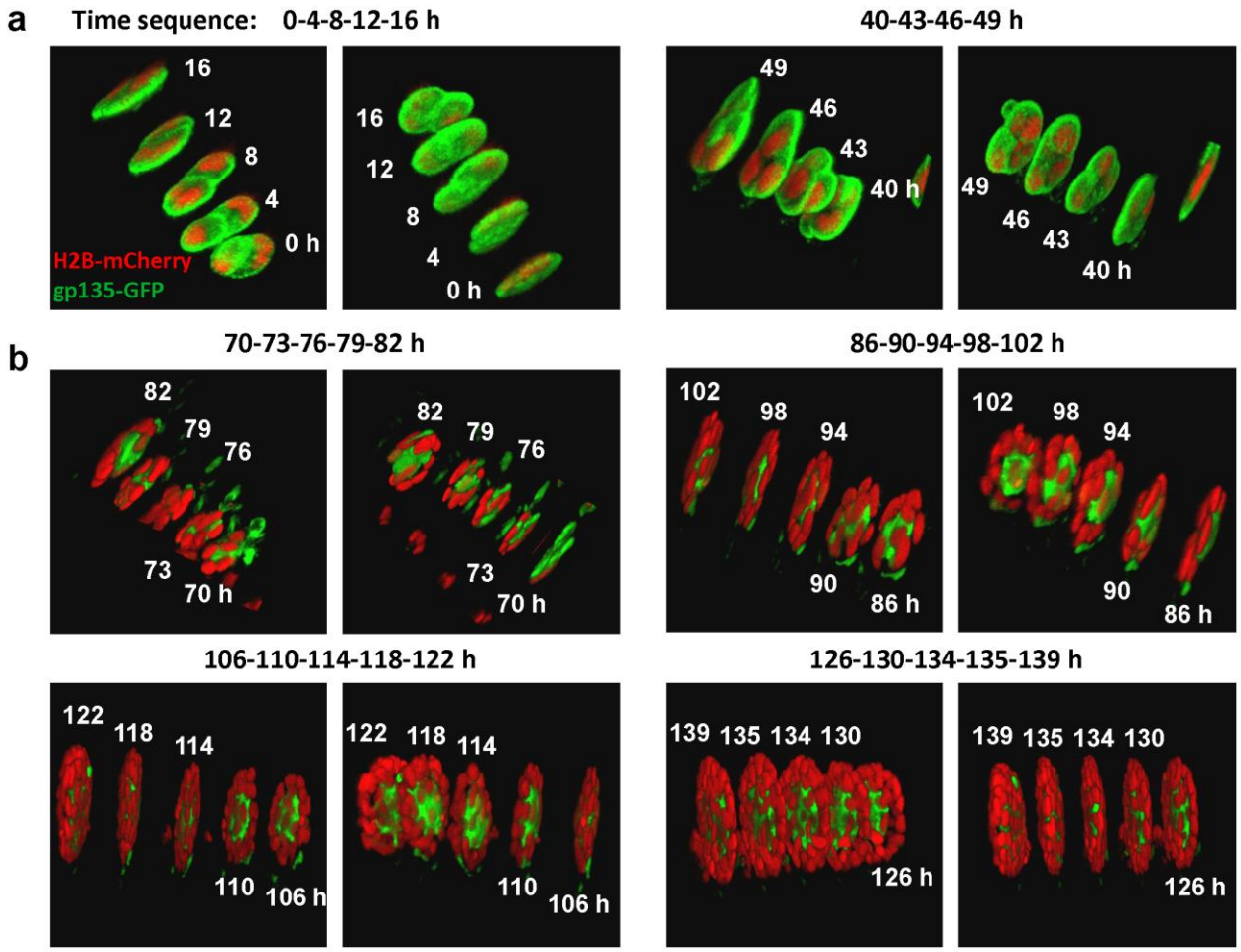

Figure 4 | The expansion of dividing cells into polarized lobule. The MCDK cells expressing gp135-GFP and H2B-mCherry were seeded on BM Matrigel gel with 2% BM in medium, and two-photon confocal imaging started one day later. The wavelengths of excitation light were 890 nm for GFP and ~1100 nm for mCherry, the step size in z-direction was 1.0 μm, and the interval time was 3 or 4 h. Medium was changed every day along with corrections of the focus and positions during the time-lapse imaging. Acquired confocal images were processed by two channels (GFP, mCherry) overlay and 3-D reconstructions. Each image here shows the 3-D view of 4 or 5 time-points at the labeled time (in hours, and the imaging starting time was set as zero), and two images for each representative time point were displayed from different angles of the 3-

bioRxiv preprint doi: https://doi.org/10.1101/2020.05.12.090068; this version posted June 19, 2020. The copyright holder for this preprint (which was not certified by peer review) is the author/funder, who has granted bioRxiv a license to display the preprint in perpetuity. It is made available under aCC-BY-NC-ND 4.0 International license.

D view. **(a)** The polarity distribution at early stage in the cluster with a few cells. **(b)** The polarity distribution during growth of the cluster into fine 3-D lobular structure. More detailed 3-D views of the polarization and cluster growth are shown in Movie 5. A note: the images of (a, b) were acquired at the same position in one experiment, but not sure whether from the exact same sample during the re-focusing process (cells were much motile at the early stage).

Culture of lobular and tubular epithelial structures under suspension conditions

The results above suggest two distinct, ECM-dependent processes to coordinate epithelial morphogenesis in the fluidic phase. The first is that cells recruit soluble BM components which are known to form branched networks[33], to create a closed-end (i.e., restricted) scaffold surrounding individual cluster. Such scaffold provides a physical barrier to block the coalescence of clusters and allow them to proliferate and polarize within the restricted space (Fig. 3a). The second process is that cells recruit soluble COL, which is known to form linear, bundled fibers[34; 35], to create an open-ended (i.e., unrestricted) scaffold (Fig. 3f). In contrast to the first one, scaffold formed by soluble COL allows clusters to continuously merge with one another through long-range interactions in the fluidic/semi-fluidic phase.

These two processes were observed in the essays where cells were supported by pre-assembled ECM, i.e., a solid phase. To ascertain whether the solid phase is absolutely required in soluble ECM-mediated epithelial cell polarization and morphogenesis, we repeated the assay in a suspension system, where agarose gel was used to replace the solid phase and minimize cell-substrate interaction (Fig. 5a) (details seen in Methods). Cells (final concentration of ~$1x10^4$ cells/ml) were mixed with medium containing no ECM (as the control) or soluble ECM

bioRxiv preprint doi: https://doi.org/10.1101/2020.05.12.090068; this version posted June 19, 2020. The copyright holder for this preprint (which was not certified by peer review) is the author/funder, who has granted bioRxiv a license to display the preprint in perpetuity. It is made available under aCC-BY-NC-ND 4.0 International license.

components (2% BM or 20 μg/ml COL), spread in the suspension system, and examined for polarization after 7-14 days.

Without soluble ECM components, cells in the suspension system were found to form clusters with a reverse polarity (i.e., gp135 located at the outer boundaries of clusters, Fig. 5b left panel), which is consistent with the previous finding [36]. By contrast, cells mixed with soluble ECM components formed structures of polarized epithelium (Fig. 5b, middle and right). Specifically, cells formed polarized lobular structures with BM (Fig. 5b middle panel) and polarized tubular structures with COL (Fig. 5b right panel), with the epithelial polarity indicated by the spatial distributions of H2B-mCherry and gp135-GFP signals (Fig. 5c(i-iii)). We noticed that under suspension culture with COL, separated small rooms (multi-lumens) were formed in the tube during polarization (Fig. 5b&e), instead of homogenous polarity through the tube on solid Matrigel (Fig. 1b), which may reflect certain different ECM microenviroments in the two culture systems. Specifically, the cells & ECM scaffolds floated in the medium during suspension culture, whereas during culture on the solid Matrigel, the ECM scaffold was bounded to hard glass surface.

Laminin immuno-staining showed the distribution of ECM scaffold around the polarized lumen (Fig. 5d), and laminin only covered the lateral sides of lobules, not at their top or bottom sides (Fig. 5d (right), Movie 6), which seemed similar to the results found in the lobules cultured on top of BM gels (Fig. 3c&d). It was noted that soluble BM and COL in the medium could self-assemble into scaffolds (Fig. 5b&d), which assisted the formation of polarized epithelium. Thus, cell-ECM interactions are required to initiate epithelial morphogenesis and create polarization at the tissue scale.

bioRxiv preprint doi: https://doi.org/10.1101/2020.05.12.090068; this version posted June 19, 2020. The copyright holder for this preprint (which was not certified by peer review) is the author/funder, who has granted bioRxiv a license to display the preprint in perpetuity. It is made available under aCC-BY-NC-ND 4.0 International license.

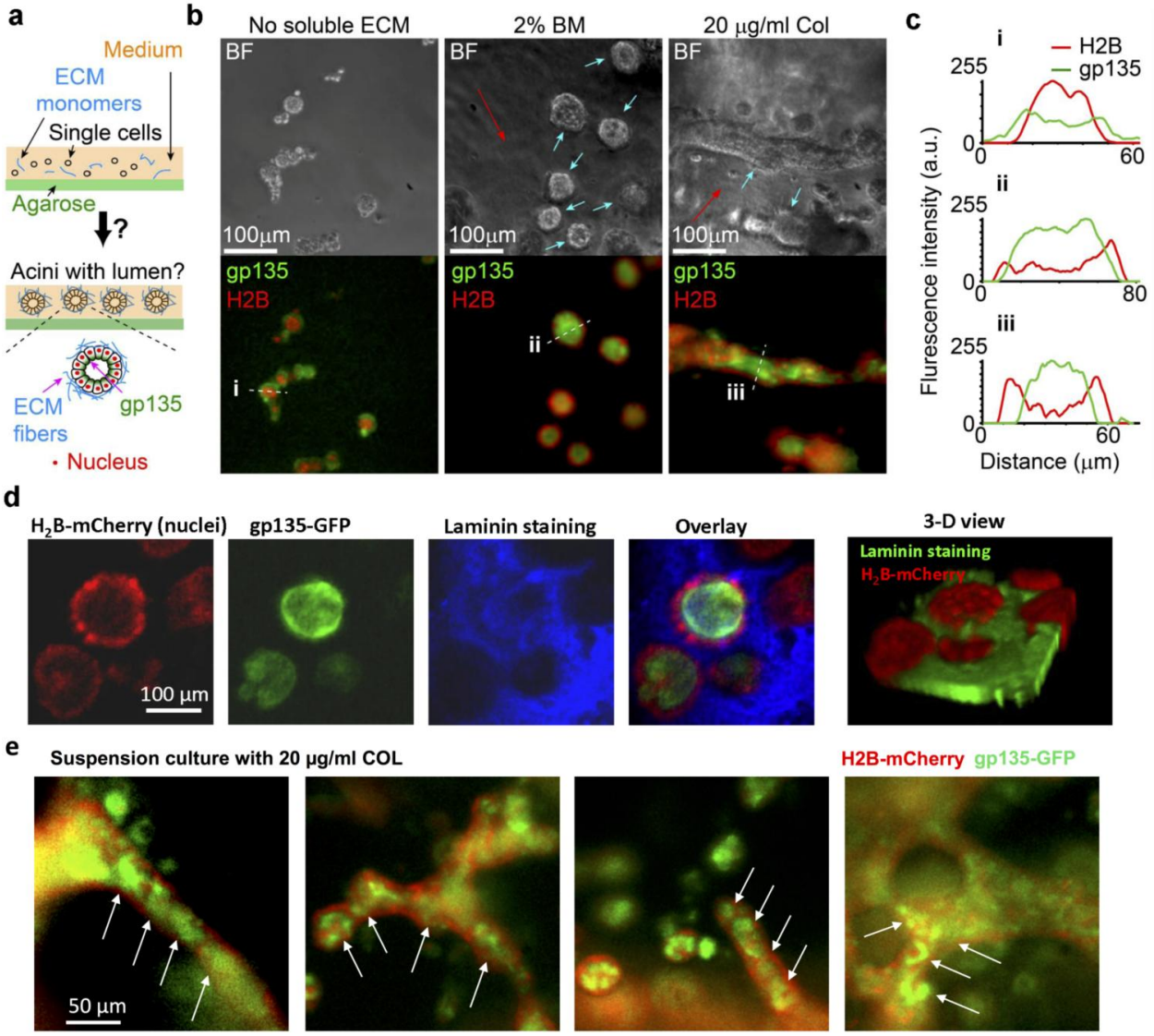

Figure 5 | Cells form tubular and lobular structures above non-adhesive substrates. (a) The design of suspension culture on agarose gel. Details are described in Methods. **(b)** Representative bright-field and 3-D projected epifluorescence images (Green: gp135, Red: H2B) for MDCK cells cultured in medium containing no ECM materials (Left), 2% BM (Middle), or 20 μg/ml COL components (Right) above 1% agarose gel for 12 days. Initial cell density: ~10^4 cells/ml. To enhance visualization, out-of-focus signals were removed and only fluorescence signals from cells near the focal plane (indicated by blue arrows) were shown. The red arrows indicated the

bioRxiv preprint doi: https://doi.org/10.1101/2020.05.12.090068; this version posted June 19, 2020. The copyright holder for this preprint (which was not certified by peer review) is the author/funder, who has granted bioRxiv a license to display the preprint in perpetuity. It is made available under aCC-BY-NC-ND 4.0 International license.

scaffolds self-assembled from soluble BM or COL. **(c)** Fluorescence intensities of H2B-mCherry and gp135-GFP along the white dotted lines (from left to right) in the indicated H2B / gp135 overlay. A cell nucleus (red) located outside the apical marker (green) indicates polarity formation. **(d)** The 3-D projected images of globules from suspension culture with 2% BM. The laminin staining (blue) indicated the assembled scaffolds from soluble BM under suspension. The images were taken by confocal microscopy (20x objective). 3-D projection of the images was obtained by collecting pixels with the maximal intensity through the entire z-stack into a single plane, and the 3-D view was constructed by the software ImageJ. **(e)** Formation of multi-lumen polarity on the tubes under suspension culture. MDCK cells were cultured above agarose gel with 20 μg/ml COL in the medium for ~two weeks. The arrows indicate some of these small lumens on the tubes.

Discussion

Emerging evidence suggests that cell-ECM interactions are crucial in regulating tissue development, homeostasis, and repair[7; 37; 38]. Such interactions can occur on the solid phase (i.e., the existing ECM scaffold) and in the fluidic phase where cells interact with soluble ECM components. Here, we showed the following findings based on the engineered MDCK cells stably co-expressing H2B-mCherry (nucleus) and gp135-EGFP (apical marker): (1) the topology of native ECM components from cells-mediated assembly helps define the morphology of epithelium tissue; (2) during tubulogenesis in the presence of soluble COL, the apicobasal polarization may start at local regions and proceed in a collective way along the axis of tubule; (3) in the fluidic phase, cells can form apicobasal polarity throughout the entire lobule/tubule with ECM only covering the lateral side (i.e. without a complete coverage of ECM at the basal side), likely resulted from the expansion process that the polarization occurs at early stage and is

bioRxiv preprint doi: https://doi.org/10.1101/2020.05.12.090068; this version posted June 19, 2020. The copyright holder for this preprint (which was not certified by peer review) is the author/funder, who has granted bioRxiv a license to display the preprint in perpetuity. It is made available under aCC-BY-NC-ND 4.0 International license.

maintained through the growth of clusters in fine 3-D structures; (4) under suspension culture with COL, the polarization was impaired by forming multi-lumens on the tubes, suggesting the importance of ECM microenvironment for tubulogenesis.

Self-organization of polarized epithelium in the fluidic phase

First in our culture system, it is the scaffold formed by cell-ECM interactions in the fluidic phase plays important roles in epithelial polarization and morphogenesis. This enables the self-assembly of polarized epithelium. We note that 3-D culture embedded in BM gels can form polarized lobules[12], and has been used as a "3-D model" to study the polarization of cells obtained from tubular organs including the kidney, the liver, and the prostate[3; 39; 40]. Such 3-D model is different from our open-system setup. In our setup, soluble ECM components secreted by cells are diluted, whereas in the 3-D model, they remain trapped within the space occupied by the cells. In turn, cell-soluble ECM interactions are allowed in the 3-D model. Indeed, ECM components secreted from cells or degraded from gels is required for epithelial polarization in the 3-D model[9; 41]. Consistently in the modified 3-D model (developed by Brugge et al.[20]) where cells are cultured on BM gels (mimicked by Matrigel in experiments), soluble BM is required for cells to form polarized lobules[5; 11; 42; 43]. These observations highlight the criticalness of cell-ECM interactions from the fluidic phase for epithelial polarization.

In general, soluble ECM can be assembled into scaffolds by ECM self-assembly and/or by cell-mediated nucleation process. The extent of cell-soluble ECM interactions in scaffold assembly depends on the cell density and the soluble ECM concentration. In our open-system setup, the concentration of soluble ECM is set low to eliminate or attenuate ECM self-assembly. By

bioRxiv preprint doi: https://doi.org/10.1101/2020.05.12.090068; this version posted June 19, 2020. The copyright holder for this preprint (which was not certified by peer review) is the author/funder, who has granted bioRxiv a license to display the preprint in perpetuity. It is made available under aCC-BY-NC-ND 4.0 International license.

contrast, the 3-D model in previous studies[12] used high concentrations of soluble ECM components to induce ECM self-assembly.

It is likely that ECM scaffolds assembled by cell-soluble ECM interactions possess a more physiological structure. For example, BM gels assembled in the absence of cells were found more resistant to laminin staining than those assembled by cells, as indicated by the difference of laminin staining (Fig. 3a), which might result from difference of porosity. Indeed, previous reports showed that immune-staining of cells in BM or COL gels requires a pre-cleavage of gels by ECM proteinases[9; 42].

Coordination of cell dynamics dependent on soluble ECM components

Our second finding is the distinct coordination of cell positioning and polarization in response to soluble BM (diluted Matrigel solution) and COL. With soluble COL, for all the experiments performed in this study, cell polarization was always found to arise after the formation of long-range structures. Here, the long-range structure is defined if cells form a spatially anisotropic organization with the longest length of principle axes > 200 μm (twice of the average diameter of polarized, lobular lumens) and the shortest length < 100 μm. By contrast, with soluble BM, cell polarization can occur without fusion of individual clusters. In addition, while cell polarization in soluble BM occurs almost simultaneously within the same cluster, cell polarization in soluble COL appears to follow a nucleation process in the cluster (Fig. 2d&f, Movies 2&3). This collective polarization proceeded along the epithelial tubule (Fig. 2g) might suggest existing intercellular signal communications at the cell-population level during tubulogenesis. The selection of topology in the polarized epithelial clusters appears to correlate with the native topology of BM and COL (i.e., lobular or linear/tubular). At this stage, nevertheless, we didn't

bioRxiv preprint doi: https://doi.org/10.1101/2020.05.12.090068; this version posted June 19, 2020. The copyright holder for this preprint (which was not certified by peer review) is the author/funder, who has granted bioRxiv a license to display the preprint in perpetuity. It is made available under aCC-BY-NC-ND 4.0 International license.

investigate how cell-soluble BM/COL interactions lead to distinct dynamics in polarity formation.

Epithelial polarization with or without direct cell-ECM contact

Our third finding is that cells can polarize without a complete coverage of ECM scaffold around the lobular/tubular structures (Figs. 3 & 5d), suggesting that some cells can maintain polarity without direct cell-ECM interactions. Nevertheless, without ECM, cells were unable to form polarity (Fig. 1 and Movie 1). Time-sequence images from confocal microscopy indicate that cells are polarized in small cluster at early stage, and continue expanding into fine 3-D lobular structure under maintained polarization (Fig. 4), which reveals one mechanism of polarization on the entire lobules without complete ECM coverage. It is a reasonable hypothesis that those cells without ECM coverage at the top of the lobules/tubules might maintain polarized under cell-cell interactions or intercellular signaling communications, instead by induction of cell-ECM interactions, which need be confirmed from further study.

It is noted from some previous studies that the apical marker gp135 (Podocalyxin) could become polarized at two-cell stage within 24-48 h under similar lobule culture system[7; 8; 23]. This doesn't sound the case from our study in which gp135-GFP got polarized at multi-cell stage after cultured for more than 48 h as visualized from both time-lapse epifluorescence microscopy and confocal scanning microscopy (seen in Fig. 2d, Fig. 4, and Movies 2&5). Although we don't have exact explanation for the difference yet, one possible reason could be that the engineered MDCK cells co-expressing H2B-mCherry and gp135-GFP might behave some different from the wild-type cells, although the engineered cells show similar capability of epithelial morphogenesis. Actually in the previously published work, Podocalyxin (gp135) staining

bioRxiv preprint doi: https://doi.org/10.1101/2020.05.12.090068; this version posted June 19, 2020. The copyright holder for this preprint (which was not certified by peer review) is the author/funder, who has granted bioRxiv a license to display the preprint in perpetuity. It is made available under aCC-BY-NC-ND 4.0 International license.

showed polarization at two-cell stage from wild-type MDCK cells (its Figure 1), whereas polarization occurred at multi-cell cluster in the engineered cells (its Movie S2)[23], consistently with our observations. Regarding gp135 also an important functional molecule in polarization and metastasis[27; 44; 45], its enhanced expression level from stable transfection might have impact on the timing process of polarization in the engineered cells.

Under suspension culture with addition of soluble ECM, cells developed polarized lobules (with BM) and tubules (with COL) (Fig. 5b), indicating cell-ECM interactions in directing the self-organization of epithelium. Interestingly, multiple lumens were formed on the tubes under suspension culture with COL (Fig. 5e) instead of the homogenous polarity through the tube on solid BM gel (Fig. 1b). This suggests that epithelial tubulogenesis is mediated by ECM microenvironment. Consistently from the previous report, perturbing cell mechanics by inhibition of ROCK-Myosin II pathway also resulted in multiple lumens during tubulogenesis, due to impaired cell motility[24]. The observations of multi-lumen tubes support that the apicobasal polarization is also mediated in mechanical way beside chemical signals.

In summary, our results highlight the criticalness of cell-ECM interactions in the fluidic phase for epithelial polarization and morphogenesis. Most importantly, we show how a physiological environment can spontaneously emerge through cell-soluble ECM interactions. The gradually collective polarization during tubulogenesis may imply the existence of intercellular communications among the cell group. In the fluidic phase, the polarization occurs in the small cluster at early stage and is maintained through the growth into fine epithelial structures. These findings might provide impact in understanding how epithelial cells develop and coordinate their polarity and positioning at tissue scales *in vivo*, as well as in the engineering of artificial organs for regenerative medicine *in vitro*.

bioRxiv preprint doi: https://doi.org/10.1101/2020.05.12.090068; this version posted June 19, 2020. The copyright holder for this preprint (which was not certified by peer review) is the author/funder, who has granted bioRxiv a license to display the preprint in perpetuity. It is made available under aCC-BY-NC-ND 4.0 International license.

Materials and Methods

Cell Culture, reagents, DNA constructs, and lentivirus

Cell culture medium and reagents were purchased from Invitrogen GIBCO. Madin Darby canine kidney (MDCK II) cells (from ATCC) were maintained in Advanced Dulbecco's modified Eagle's medium (serum reduced medium) supplemented with 3% fetal bovine serum, 2 mM L-glutamine, 20 unit/ml penicillin, 20 μg/ml streptomycin, and 1 mM sodium pyruvate in a humidified 95% air, 5% CO_2 incubator at 37 ℃.

BD Matrigel (basement membrane matrix, growth factor reduced, phenol red-free), and 3-D Culture Matrix™ Rat Collagen I (5 mg/ml) were purchased from BD Biosciences and R&D Systems, respectively. Rabbit anti-laminin and mouse anti-collagen I primary antibodies were purchased from Sigma. Pacific Blue-conjugated goat anti-rabbit and anti-mouse IgGs were purchased from Invitrogen.

The plasmid pcDNA3-gp135-GFP construct was a gift from Dr. Joachim Füllekrug (Max Planck Institute of Molecular Cell Biology and Genetics)[27]. The plasmid expressing GFP-tagged human β-actin (GFP-β-actin) under endogenous promoter was provided by Dr. Beat A. Imhof (Switzerland)[46]. Lentivirus encoding mCherry-conjugated histone H2B (H2B-mCherry) was generously provided by Dr. Rusty Lansford and David Huss (Biology, California Institute of Technology)[26].

Development of stable fluorescent MDCK cell lines

bioRxiv preprint doi: https://doi.org/10.1101/2020.05.12.090068; this version posted June 19, 2020. The copyright holder for this preprint (which was not certified by peer review) is the author/funder, who has granted bioRxiv a license to display the preprint in perpetuity. It is made available under aCC-BY-NC-ND 4.0 International license.

We first developed the stable MDCK cell line expressing H2B-mCherry (MDCK_H2B-mCherry). Cells at 20-30% confluency were infected with lentivirus encoding H2B-mCherry. The infected cells were then diluted in 96-well plates to enable the selection and the expansion of single fluorescent colony. Next, we transfected MDCK_H2B-mCherry cells with the plasmid construct, pcDNA3-gp135-GFP, to develop the cell line expressing H2B-mCherry and gp135-GFP (MDCK_H2B-mCherry/gp135-GFP). In addition, we have transfected MDCK cells with GFP-β-actin plasmid (MDCK_GFP-actin). This cell line was used to compare the results obtained from MDCK_H2B-mCherry/gp135-GFP cells. The transfection was performed by using Lipofectamine2000 (Invitrogen), followed by the antibiotic selection with G418 (300 ug/ml) for 2 weeks to obtain a cell pool expressing various levels of gp135-GFP. A single colony displaying an intermediate fluorescence intensity of gp135-GFP or GFP-β-actin was selected through a series of dilution, selection, and expansion of the cell pool in 96-well plates.

Chambers for cell culture and microscopy

Cell culture experiments and time-lapse microscopy were performed in home-made, stainless steel chambers. These chambers were manufactured to have a rectangular shape with a height of 0.6 cm and a 2 cm x 5.5 cm internal opening. Nail polish was used to seal 24x60 mm No. 1 cover slips on the bottom of the chambers. To perform multiple-well experiments in one chamber, polydimethylsiloxane (PDMS) blocks of a size compatible with the internal opening of the chambers were prepared and carved through to create multiple square wells (~0.5x0.5 cm^2). The surface of PDMS blocks were then cleaned and air-dried to allow for a firm contact with the coverslips of the chambers.

Cell culture on BM gels or less-adhesive substrates

bioRxiv preprint doi: https://doi.org/10.1101/2020.05.12.090068; this version posted June 19, 2020. The copyright holder for this preprint (which was not certified by peer review) is the author/funder, who has granted bioRxiv a license to display the preprint in perpetuity. It is made available under aCC-BY-NC-ND 4.0 International license.

We prepared basement membrane (BM) gels following the protocol provided by the manufacturer. The total concentration of proteins in original growth factors-reduced (GFR) BD Matrigel stock solution is ~10 mg/ml. The major components are laminin (~61%), collagen IV (~30%) and Entactin (~7%). To make BM gels, we first prepared chambers sealed with coverslips on the bottom. The stock solution (100%) of BD Matrigel (stored at 4 ℃) was then spread on the top of the coverslips (40-80 μl/cm^2) at 37 ℃ for 20-30 min. This allowed the stock solution to form a layer of gel with a variable height (200-400 μm).

To place cells, we prepared culture medium containing 2% soluble BM (20 μl of Matrigel solution per 1 ml of medium) or 20 μg/ml type I collagen (COL) at 4 ℃. Individual MDCK cells (~1-2 ×10^4 cells/cm^2) were seeded on the top of BM gels in the culture medium containing 2% BM or 20 μg/ml COL. The seeding cell density of ~1-2 ×10^4 cells/cm^2 on Matrigel was chosen from experimental testing, which were suitable for both lobular and tubular structure formation. We then placed the chamber in a petri dish in a 37 ℃ incubator and changed the medium every 4 days, (or every day or every other day under time-lapse microscopy). Here, the concentration of BM in the medium followed the "on-top" assay developed by Bissell and her coworkers[47]. For the concentration of COL in the medium, we used 20 μg/ml because COL at 1 mg/ml forms gels with rigidity compatible to 100% BM gels[19]. Nevertheless, we have varied the concentrations of COL in the medium from 5 to 50 μg/ml. Within this range, COL was not found to form gels and cells could form tubule-like structures (at an initial cell density ~10^4 cells/cm^2) with COL.

For cell culture on less-adhesive substrates, we first prepared a layer of agarose gel (1%) on top of coverslips of the chambers. A mixture of MDCK cells (~10^4 cells/ml) and culture medium containing 2% BM or 20 μg/ml COL was added to the chambers. We then placed the chamber in a petri dish in 37 ℃ incubator. To minimize the evaporation, the chambers were covered by

bioRxiv preprint doi: https://doi.org/10.1101/2020.05.12.090068; this version posted June 19, 2020. The copyright holder for this preprint (which was not certified by peer review) is the author/funder, who has granted bioRxiv a license to display the preprint in perpetuity. It is made available under aCC-BY-NC-ND 4.0 International license.

coverslips with a small opening (~5 mm) to allow for air exchange. Medium was changed carefully every 7 days without destroying or losing the cell aggregates in the medium.

Immuno-staining experiments

Immuno-staining experiments were conducted at room temperature, except the step of incubation with primary antibodies. In brief, cell samples were fixed in 4% paraformaldehyde for 15 min, and permeabilized with 0.1% Triton X-100 for 20 min. The cells were then incubated with rabbit anti-laminin or mouse anti-collagen I primary antibody overnight at 4 ℃, followed by incubation with goat secondary antibody conjugated with Pacific Blue (410/455 nm) for 2 hours. The images were collected by using epifluorescence or scanning microscopy.

Epifluorescence and scanning microscopy

Olympus IX71 were equipped with automatic XYZ stages (MS-2000, ASI) and piezo-electric objective stages (P-721 Pifoc, Physik Instrumente) for fast multi-position, z-scanning, and auto-focusing time-lapse epifluorescence microscopy. An environmental chamber (Haison) was used to maintain humidity, CO_2 concentration (5%), and temperature (37 ℃). For phase-contrast and/or epi-fluorescence microscopy, the imaging system based on Olympus IX71 microscope was equipped with motorized excitation and emission filters with a shutter control (lambda 10-3, Sutter), an Electron-Multiplying CCD camera (ImagEM, C9100-13, Hamamatsu, 512 × 512 pixels, water cooled to -95°C), and a 120W fluorescent illumination lamp (X-CITE 120Q, EXFO, Lumen Dynamics Group Inc.). For confocal scanning microscopy, the microscope was equipped with lasers with three wavelengths (405nm, 475nm and 594nm), photomultiplier tubes (H10425 and H7422-40, Hamamatsu). The two-photon scanning microscope set up on Olympus IX71 was

bioRxiv preprint doi: https://doi.org/10.1101/2020.05.12.090068; this version posted June 19, 2020. The copyright holder for this preprint (which was not certified by peer review) is the author/funder, who has granted bioRxiv a license to display the preprint in perpetuity. It is made available under aCC-BY-NC-ND 4.0 International license.

equipped with a Mai-Tai™ femtosecond laser source (Spectra-Physics). 20x objective (NA: 0.45, Olympus) and 10x objective (NA: 0.3, Olympus) were used in the experiments.

Image acquisition and analysis

For phase-contrast and/or epifluorescence timelapse microscopy, Metamorph (version 7.7.3) was used to control the devices and the image acquisition. To acquire z-stack, epifluorescent images were taken at 21 planes with a step size 4.5 μm. 3-D projection was obtained by collecting pixels with the maximal intensity through the entire z-stack into a single plane (through metamorph or matlab programming). For scanning microscopy, Labview was used to run automatic scanning and image acquisition. The exposure time and gains were adjusted according to the image quality and the photo-bleaching effect. Metamorph, Labview, and ImageJ were used for image analysis.

Acknowledgement We want to thank Dr. Joachim Füllekrug (Max Planck Institute of Molecular Cell Biology and Genetics) for pcDNA3-gp135-GFP construct, and Dr. Rusty Lansford and David Huss (Biology, California Institute of Technology) for Lentivirus encoding H2B-mCherry. This work is financially supported by Ellison Medical Foundation and Western Heaven Funds (C.G.); National Natural Science Foundation of China (NSFC11872129) and Natural Science Foundation of Jiangsu Province (BK20181416) (M.O.); National Natural Science Foundation of China (NSFC11532003) (L.D.).

Author Contributions M. Ouyang and C. Guo designed the research and performed data analysis; M. Ouyang, J-Y Yu, C. Guo conducted the experiments; J-Y Yu, Y Chen, and C. Guo constructed the microscopes and developed the imaging programs; L Deng provided discussion and certain fund support; M. Ouyang, C. Guo and L. Deng prepared the manuscript.

Conflict of Interest: the authors declare no conflict of interest in this work.

bioRxiv preprint doi: https://doi.org/10.1101/2020.05.12.090068; this version posted June 19, 2020. The copyright holder for this preprint (which was not certified by peer review) is the author/funder, who has granted bioRxiv a license to display the preprint in perpetuity. It is made available under aCC-BY-NC-ND 4.0 International license.

References

[1] S. Quintin, C. Gally, and M. Labouesse, Epithelial morphogenesis in embryos: asymmetries, motors and brakes. Trends Genet 24 (2008) 221-30.

[2] D.M. Bryant, and K.E. Mostov, From cells to organs: building polarized tissue. Nat Rev Mol Cell Biol 9 (2008) 887-901.

[3] F. Martin-Belmonte, and K. Mostov, Regulation of cell polarity during epithelial morphogenesis. Curr Opin Cell Biol 20 (2008) 227-34.

[4] D. St Johnston, and J. Ahringer, Cell polarity in eggs and epithelia: parallels and diversity. Cell 141 (2010) 757-74.

[5] D.M. Bryant, A. Datta, A.E. Rodriguez-Fraticelli, J. Peranen, F. Martin-Belmonte, and K.E. Mostov, A molecular network for de novo generation of the apical surface and lumen. Nat Cell Biol 12 (2010) 1035-45.

[6] J. Cait, M.R. Hughes, M.R. Zeglinski, A.W. Chan, S. Osterhof, R.W. Scott, D. Canals Hernaez, A. Cait, A.W. Vogl, P. Bernatchez, T.M. Underhill, D.J. Granville, T.H. Murphy, C.D. Roskelley, and K.M. McNagny, Podocalyxin is required for maintaining blood-brain barrier function during acute inflammation. Proc Natl Acad Sci U S A 116 (2019) 4518-4527.

[7] K. Klinkert, M. Rocancourt, A. Houdusse, and A. Echard, Rab35 GTPase couples cell division with initiation of epithelial apico-basal polarity and lumen opening. Nature communications 7 (2016) 11166.

[8] P.S. Mrozowska, and M. Fukuda, Regulation of podocalyxin trafficking by Rab small GTPases in 2D and 3D epithelial cell cultures. J Cell Biol 213 (2016) 355-69.

[9] L.E. O'Brien, T.S. Jou, A.L. Pollack, Q. Zhang, S.H. Hansen, P. Yurchenco, and K.E. Mostov, Rac1 orientates epithelial apical polarity through effects on basolateral laminin assembly. Nat Cell Biol 3 (2001) 831-8.

[10] W. Yu, A. Datta, P. Leroy, L.E. O'Brien, G. Mak, T.S. Jou, K.S. Matlin, K.E. Mostov, and M.M. Zegers, Beta1-integrin orients epithelial polarity via Rac1 and laminin. Mol Biol Cell 16 (2005) 433-45.

[11] F. Martin-Belmonte, A. Gassama, A. Datta, W. Yu, U. Rescher, V. Gerke, and K. Mostov, PTEN-mediated apical segregation of phosphoinositides controls epithelial morphogenesis through Cdc42. Cell 128 (2007) 383-97.

[12] R.J. Blaschke, A.R. Howlett, P.Y. Desprez, O.W. Petersen, and M.J. Bissell, Cell differentiation by extracellular matrix components. Methods Enzymol 245 (1994) 535-56.

[13] D.J. Dickinson, W.J. Nelson, and W.I. Weis, A polarized epithelium organized by beta- and alpha-catenin predates cadherin and metazoan origins. Science 331 (2011) 1336-9.

[14] A.A. Mailleux, M. Overholtzer, and J.S. Brugge, Lumen formation during mammary epithelial morphogenesis: insights from in vitro and in vivo models. Cell Cycle 7 (2008) 57-62.

[15] W.J. Nelson, Adaptation of core mechanisms to generate cell polarity. Nature 422 (2003) 766-74.

[16] T. Rozario, and D.W. DeSimone, The extracellular matrix in development and morphogenesis: a dynamic view. Dev Biol 341 (2010) 126-40.

[17] E. Dhimolea, M.V. Maffini, A.M. Soto, and C. Sonnenschein, The role of collagen reorganization on mammary epithelial morphogenesis in a 3D culture model. Biomaterials 31 (2010) 3622-30.

[18] M.A. Wozniak, R. Desai, P.A. Solski, C.J. Der, and P.J. Keely, ROCK-generated contractility regulates breast epithelial cell differentiation in response to the physical properties of a three-dimensional collagen matrix. J Cell Biol 163 (2003) 583-95.

bioRxiv preprint doi: https://doi.org/10.1101/2020.05.12.090068; this version posted June 19, 2020. The copyright holder for this preprint (which was not certified by peer review) is the author/funder, who has granted bioRxiv a license to display the preprint in perpetuity. It is made available under aCC-BY-NC-ND 4.0 International license.

[19] M.J. Paszek, N. Zahir, K.R. Johnson, J.N. Lakins, G.I. Rozenberg, A. Gefen, C.A. Reinhart-King, S.S. Margulies, M. Dembo, D. Boettiger, D.A. Hammer, and V.M. Weaver, Tensional homeostasis and the malignant phenotype. Cancer Cell 8 (2005) 241-54.

[20] S.K. Muthuswamy, D. Li, S. Lelievre, M.J. Bissell, and J.S. Brugge, ErbB2, but not ErbB1, reinitiates proliferation and induces luminal repopulation in epithelial acini. Nat Cell Biol 3 (2001) 785-92.

[21] C.L. Guo, M. Ouyang, J.Y. Yu, J. Maslov, A. Price, and C.Y. Shen, Feature Article: From the Cover: Long-range mechanical force enables self-assembly of epithelial tubular patterns. Proceedings of the National Academy of Sciences of the United States of America 109 (2012) 5576-82.

[22] P. Ekblom, K. Alitalo, A. Vaheri, R. Timpl, and L. Saxen, Induction of a basement membrane glycoprotein in embryonic kidney: possible role of laminin in morphogenesis. Proc Natl Acad Sci U S A 77 (1980) 485-9.

[23] D.M. Bryant, J. Roignot, A. Datta, A.W. Overeem, M. Kim, W. Yu, X. Peng, D.J. Eastburn, A.J. Ewald, Z. Werb, and K.E. Mostov, A molecular switch for the orientation of epithelial cell polarization. Developmental cell 31 (2014) 171-87.

[24] M. Kim, M.S. A, A.J. Ewald, Z. Werb, and K.E. Mostov, p114RhoGEF governs cell motility and lumen formation during tubulogenesis through a ROCK-myosin-II pathway. Journal of cell science 128 (2015) 4317-27.

[25] J. Wang, J. Guo, B. Che, M. Ouyang, and L. Deng, Cell motion-coordinated fibrillar assembly of soluble collagen I to promote MDCK cell branching formation. Biochem Biophys Res Commun 524 (2020) 317-324.

[26] Y. Sato, G. Poynter, D. Huss, M.B. Filla, A. Czirok, B.J. Rongish, C.D. Little, S.E. Fraser, and R. Lansford, Dynamic analysis of vascular morphogenesis using transgenic quail embryos. PLoS One 5 (2010) e12674.

[27] D. Meder, A. Shevchenko, K. Simons, and J. Fullekrug, Gp135/podocalyxin and NHERF-2 participate in the formation of a preapical domain during polarization of MDCK cells. J Cell Biol 168 (2005) 303-13.

[28] G. Parry, E.Y. Lee, D. Farson, M. Koval, and M.J. Bissell, Collagenous substrata regulate the nature and distribution of glycosaminoglycans produced by differentiated cultures of mouse mammary epithelial cells. Exp Cell Res 156 (1985) 487-99.

[29] T.W. Ecay, and J.D. Valentich, Basal lamina formation by epithelial cell lines correlates with laminin A chain synthesis and secretion. Exp Cell Res 203 (1992) 32-8.

[30] A.I. Ivanov, A.M. Hopkins, G.T. Brown, K. Gerner-Smidt, B.A. Babbin, C.A. Parkos, and A. Nusrat, Myosin II regulates the shape of three-dimensional intestinal epithelial cysts. Journal of cell science 121 (2008) 1803-14.

[31] R. Kalluri, Basement membranes: structure, assembly and role in tumour angiogenesis. Nat Rev Cancer 3 (2003) 422-33.

[32] K. Mostov, P. Brakeman, A. Datta, A. Gassama, L. Katz, M. Kim, P. Leroy, M. Levin, K. Liu, F. Martin, L.E. O'Brien, M. Verges, T. Su, K. Tang, N. Tanimizu, T. Yamaji, and W. Yu, Formation of multicellular epithelial structures. Novartis Found Symp 269 (2005) 193-200; discussion 200-5, 223-30.

[33] D.E. Ingber, Mechanical control of tissue morphogenesis during embryological development. Int J Dev Biol 50 (2006) 255-66.

[34] T. Starborg, Y. Lu, R.S. Meadows, K.E. Kadler, and D.F. Holmes, Electron microscopy in cell-matrix research. Methods 45 (2008) 53-64.

[35] K.E. Kadler, A. Hill, and E.G. Canty-Laird, Collagen fibrillogenesis: fibronectin, integrins, and minor collagens as organizers and nucleators. Curr Opin Cell Biol 20 (2008) 495-501.

bioRxiv preprint doi: https://doi.org/10.1101/2020.05.12.090068; this version posted June 19, 2020. The copyright holder for this preprint (which was not certified by peer review) is the author/funder, who has granted bioRxiv a license to display the preprint in perpetuity. It is made available under aCC-BY-NC-ND 4.0 International license.

[36] A.Z. Wang, G.K. Ojakian, and W.J. Nelson, Steps in the Morphogenesis of a Polarized Epithelium .1. Uncoupling the Roles of Cell Cell and Cell Substratum Contact in Establishing Plasma-Membrane Polarity in Multicellular Epithelial (Mdck) Cysts. Journal of cell science 95 (1990) 137-151.

[37] S.J. Sequeira, M. Larsen, and T. DeVine, Extracellular matrix and growth factors in salivary gland development. Front Oral Biol 14 (2010) 48-77.

[38] D.J. Behonick, and Z. Werb, A bit of give and take: the relationship between the extracellular matrix and the developing chondrocyte. Mech Dev 120 (2003) 1327-36.

[39] M.M. Webber, D. Bello, H.K. Kleinman, and M.P. Hoffman, Acinar differentiation by non-malignant immortalized human prostatic epithelial cells and its loss by malignant cells. Carcinogenesis 18 (1997) 1225-31.

[40] N. Tanimizu, A. Miyajima, and K.E. Mostov, Liver progenitor cells develop cholangiocyte-type epithelial polarity in three-dimensional culture. Mol Biol Cell 18 (2007) 1472-9.

[41] G.E. Davis, W. Koh, and A.N. Stratman, Mechanisms controlling human endothelial lumen formation and tube assembly in three-dimensional extracellular matrices. Birth Defects Res C Embryo Today 81 (2007) 270-85.

[42] S.H. Kim, S. Park, K. Mostov, J. Debnath, and C.A. Hunt, Computational investigation of epithelial cell dynamic phenotype in vitro. Theor Biol Med Model 6 (2009) 8.

[43] A. Datta, D.M. Bryant, and K.E. Mostov, Molecular regulation of lumen morphogenesis. Curr Biol 21 (2011) R126-36.

[44] J. Frose, M.B. Chen, K.E. Hebron, F. Reinhardt, C. Hajal, A. Zijlstra, R.D. Kamm, and R.A. Weinberg, Epithelial-Mesenchymal Transition Induces Podocalyxin to Promote Extravasation via Ezrin Signaling. Cell reports 24 (2018) 962-972.

[45] K.A. Snyder, M.R. Hughes, B. Hedberg, J. Brandon, D.C. Hernaez, P. Bergqvist, F. Cruz, K. Po, M.L. Graves, M.E. Turvey, J.S. Nielsen, J.A. Wilkins, S.R. McColl, J.S. Babcook, C.D. Roskelley, and K.M. McNagny, Podocalyxin enhances breast tumor growth and metastasis and is a target for monoclonal antibody therapy. Breast Cancer Res 17 (2015) 46.

[46] C. Ballestrem, B. Wehrle-Haller, and B.A. Imhof, Actin dynamics in living mammalian cells. Journal of cell science 111 (Pt 12) (1998) 1649-58.

[47] G.Y. Lee, P.A. Kenny, E.H. Lee, and M.J. Bissell, Three-dimensional culture models of normal and malignant breast epithelial cells. Nat Methods 4 (2007) 359-65.